Quantum Electronics **48** (9) 849–853 (2018)

TERAHERTZ RADIATION

https://doi.org/10.1070/QEL16704

Continuous-wave laser generation of slow THz surface plasmons in an array of single-walled carbon nanotubes

S.A. Afanas'ev, I.O. Zolotovskii, A.S. Kadochkin, S.G. Moiseev, V.V. Svetukhin, A.A. Pavlov

Abstract. **The mechanism of generation of surface plasmon polaritons in the THz and far-IR ranges by laser irradiation of arrays of single-walled carbon nanotubes is considered. It is shown that by varying the angle of incidence of the laser beam, one can change the frequency of generated surface plasmon polaritons. As consequence, the nanotube length can be matched to the laser wavelength for efficient conversion of cw laser radiation to the THz range.**

Keywords: *terahertz radiation, single-walled carbon nanotubes, surface plasmon polaritons.*

1. Introduction

Currently, the design of compact room-temperature generators of electromagnetic terahertz (THz) radiation (with wavelengths in the range of 0.1–3 mm), fit for various practical applications in spectroscopy, medical diagnostics, safety systems, and other fields of science and technology, is an urgent problem [1–4].

Modern THz radiation sources can arbitrarily be divided into two large groups. The first includes electron-vacuum sources: backward-wave tubes, X-ray free-electron lasers, bremsstrahlung generators (from linear accelerators to synchrotrons), gyrotrons, and orotrons [2, 5]. The second group contains solid-state sources: parametric oscillators and generators based on frequency multiplication in semiconductor laser diodes and waveguides [6], multilayer quantum-cascade heterostructures [7], Gunn diodes and high-frequency transistors, Josephson oscillators [8], and converters based on optical rectification effect [9–13]. In the latter case, optical pumping is performed by a pulsed laser, and the target where laser pulses are subjected to optical rectification is a semiconductor structure. Various plasmonic structures, quantum dots, and other objects can be formed in the target in order to increase its conversion efficiency. Since a short laser pulse has a wide spectrum, only a small part of energy is converted into THz radiation; generally, the conversion efficiency does not exceed 10^{-5}–10^{-6} [10].

The laser-to-THz conversion efficiency can be increased using schemes implementing cw wavelength conversion. An example is the scheme based on two counterpropagating laser beams with THz detuning, which irradiate a composite containing carbon nanotubes (CNTs) [14]; in this configuration, field beatings occur at the corresponding frequency. However, in this case one must provide beam locking for two independent laser sources. As was indicated in [14], the conversion efficiency of this scheme may amount to 10^{-6}, i.e., be comparable with the efficiencies typical of the pulsed scheme or even lower [10–13].

In this study, we suggest a scheme of a THz generator based on a cw laser. The mechanism of generation of slow surface plasmon polaritons (SPPs) in arrays of single-walled CNTs (SWCNTs) in the laser field is considered. The use of CNT arrays irradiated by a cw laser beam as submillimeter radiation sources is a promising line in the design of THz generators. CNT arrays and nanocomposites on their basis can successfully be used to solve various problems related to the generation of electromagnetic radiation in the THz and microwave ranges [15–26]. In particular, a CNT may serve as a transmission line (waveguide), maintaining propagation of a superslow (with an effective refractive index of more 100) surface electromagnetic wave [15, 19, 27–31].

We showed that the plasmon waves generated in a CNT array by one or two laser beams may provide generation of submillimeter radiation. The SPP generation conditions in such structures under cw laser irradiation at a wavelength of 1.06 μm (the operating wavelength of the most widespread and available fibre and solid-state laser sources with high average and peak powers) are found. The case where slow SPPs are excited in an SWCNT array under conditions of interaction of narrow-band laser radiation (incident and reflected waves) with periodically arranged CNTs is considered. Surface waves are formed due to the decay (process of the same type as the parametric three-wave interaction in a periodic structure) of the initial laser wave into a reflected wave and SPPs on the SWCNT surface. The two-beam scheme of slow SPP excitation, based on application of two laser sources with slightly differing frequencies, is also discussed. In this case, the slow SPP is generated at the difference frequency. Phase-matching conditions must be implemented for the corresponding wave processes in both schemes.

S.A. Afanas'ev, I.O. Zolotovskii, A.S. Kadochkin Ulyanovsk State University, ul. L. Tolstogo 42, 432700 Ulyanovsk, Russia;
e-mail: rafzol.14@mail.ru;
S.G. Moiseev Ulyanovsk State University, ul. L. Tolstogo 42, 432700 Ul'yanovsk, Russia; Kotelnikov Institute of Radio Engineering and Electronics (Ulyanovsk Branch), Russian Academy of Sciences, ul. Goncharova 48/2, 432011 Ulyanovsk, Russia;
e-mail: serg-moiseev@yandex.ru;
V.V. Svetukhin Ulyanovsk State University, ul. L. Tolstogo 42, 432700 Ul'yanovsk, Russia; Institute of Nanotechnology of Microelectronics, Russian Academy of Sciences, Leninsky prosp. 32a, 119991 Moscow, Russia;
A.A. Pavlov Institute of Nanotechnologies of Microelectronics, Russian Academy of Sciences, Leninsky prosp. 32a, 119991 Moscow, Russia

Received 12 April 2018; revision received 2 July 2018
Kvantovaya Elektronika **48** (9) 849–853 (2018)
Translated by Yu.P. Sin'kov

2. Statement of the problem

Let us consider a two-dimensional ordered array of identical SWCNTs with a radius a, oriented parallel and spaced by the same distance d (Fig. 1a). The nanotubes are assumed to be sufficiently long, so that the condition $d \ll L$ (L is the nanotube length) is satisfied. A laser beam with a frequency θ_1 and wave number $k_1 = \omega_1/c$ (c is the speed of light in vacuum) is incident on this periodic structure (diffraction grating) at an angle ω_1 with respect to the x axis (normal to the nanotube symmetry axes). The laser field will be approximated by a TM-polarised plane wave. The diffracted beam of lower frequency $\omega_2 = \omega_1 - \Omega$ has a wave vector $k_2 = \omega_2/c$, directed at an angle θ_2 to the x axis.

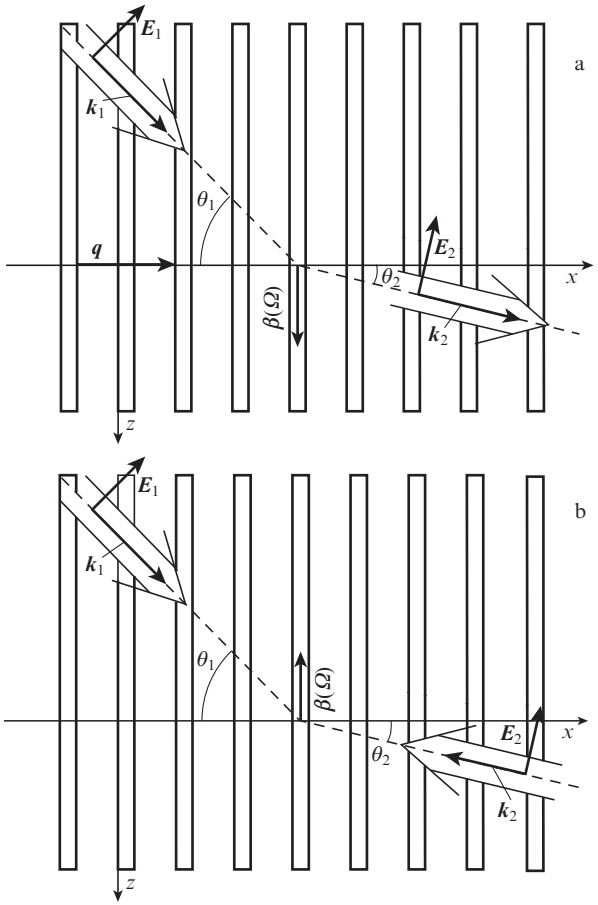

Figure 1. Geometry of the problem: the SPP generation in an SWCNT array by (a) one and (b) two laser beams.

The electric field of the incident wave with this polarisation has a component directed along the nanotubes (z axis). Its presence is necessary for the occurrence of the longitudinal component of the density vector of the current through the nanotube surface and the excitation of a slow surface wave, guided by the nanotube (which plays the role of a waveguide) [15, 19, 28–33].

The Bragg diffraction condition, with allowance for the generation of a SPP excited at the difference frequency Ω and propagating along the nanotubes (z axis) with a wave vector $\boldsymbol{\beta}$, can be written as

$$\boldsymbol{k}_1 = \boldsymbol{k}_2 + \boldsymbol{\beta}(\Omega) + \boldsymbol{q}, \tag{1}$$

where $\boldsymbol{q}$ is the periodic structure wave vector ($q = 2\pi p/d$, p is the diffraction order). Only the first-order diffraction beams with $p = \pm 1$ are taken into account below.

In the projections on the x and z axes of the introduced coordinate system, condition (1) takes the form

$$\begin{aligned} k_1\cos\theta_1 - k_2\cos\theta_2 &= q, \\ k_1\sin\theta_1 - k_2\sin\theta_2 &= \beta(\Omega). \end{aligned} \tag{2}$$

Furthermore, we analyse the conditions for the existence of solutions to system (2) and solve this system numerically for different structure periods d and angles of incidence θ_1 (in the range $0 \leqslant \theta_1 < 90°$).

3. Dispersion relation

To analyse and solve system (2), one must have a dispersion relation, i.e., the dependence $\beta(\Omega)$ for the wave vector of a SPP propagating along the nanotube axis. The electrodynamic problem of propagation of a surface wave in a waveguide formed by CNTs can be solved in different ways [15, 8–33]; however, they all yield well-consistent dependences. In this study we use the dispersion relation for a surface TM wave in a metallic SWCNT with loss disregarded, which was reported in [28]:

$$\mathrm{i}\Omega\varepsilon_0 = \sigma_{zz}\beta^2 aI(\beta a)K(\beta a). \tag{3}$$

Here, ε_0 is the permittivity of free space; $I(\beta a)$ and $K(\beta a)$ are, respectively, modified Bessel functions of the first and second kinds; and

$$\sigma_{zz} = \frac{\mathrm{i}n_0 e^2}{m_\mathrm{e}\Omega} \tag{4}$$

is the longitudinal component of the conductivity tensor of a metallic SWCNT (n_0 is the equilibrium surface density of π electrons in the CNT, e is the elementary charge, and m_e is the effective electron mass).

The ratio n_0/m_e entering (4) was estimated in [34] as follows:

$$\frac{n_0}{m_\mathrm{e}} = \frac{2V_\mathrm{F}}{\pi^2\hbar a}, \tag{5}$$

where $\hbar$ is Planck's constant and V_F is the Fermi velocity, whose value for metallic SWCNTs is estimated to be $(0.9–1) \times 10^6$ m s^{-1} [29].

Figure 2 shows dependences $\beta(\Omega)$, calculated from formulas (3)–(5) for different nanotube radii, and the corresponding frequency dependences of phase velocity $V_\mathrm{ph} = \Omega/\beta$. The dependence $\beta(\Omega)$ can be considered as linear with a high accuracy in the frequency range of interest. Specifically this approximation will be used below: we assume that $\beta = \Omega/V_\mathrm{ph}$ in (2) and take the average value of phase velocity ($V_\mathrm{ph} = 6 \times 10^6$ m/s) for a nanotube of radius $a = 1$ nm in the frequency range presented in Fig. 2.

4. Analysis of the phase-matching condition

We will search for a solution to system (2) in dependence of the angle of incidence of laser beam on the structure, θ_1, at a fixed grating period d. The following expressions for the

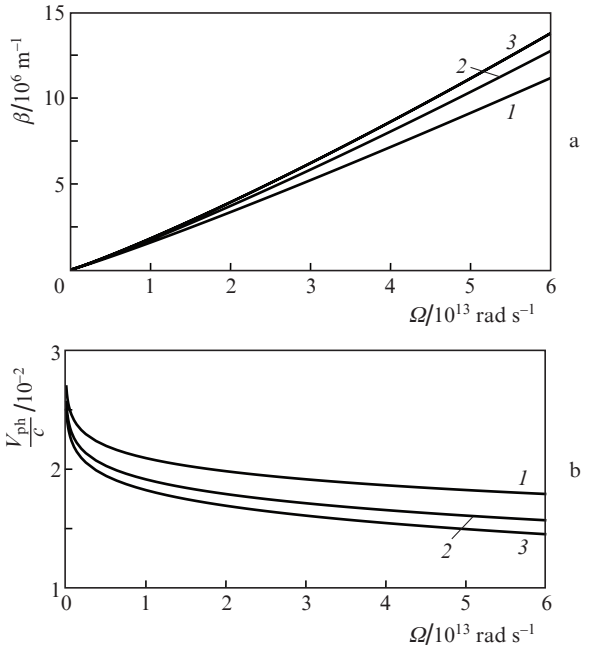

Figure 2. Frequency dependences of (a) the wave number and (b) phase velocity normalised to the speed of light; SPP in metallic SWCNTs with radii a = (*1*) 0.5, (*2*) 1.5, and (*3*) 2.5 nm.

desired angle θ_2 can be derived from the first and second equations of system (2):

$$\cos\theta_2 = \frac{k_1\cos\theta_1 - q}{k_2} = \frac{\omega_1\cos\theta_1 - qc}{\omega_1 - \Omega}, \tag{6}$$

$$\cos\theta_2 = \frac{k_1\sin\theta_1 - \beta(\Omega)}{k_2} = \frac{\omega_1\sin\theta_2 - c\beta(\Omega)}{\omega_1 - \Omega}, \tag{7}$$

which yield the following relation for Ω

$$(\omega_1 - \Omega)^2 = (\omega_1\cos\theta_1 - qc)^2 + [\omega_1\sin\theta_1 - c\beta(\Omega)]^2. \tag{8}$$

Having solved numerically (8), we find Ω and then determine the angle θ_2 from formulas (6) and (7).

Furthermore, to simplify the analysis, we assume that $\Omega \ll \omega_1$. Then Eqn (6) takes the form

$$\cos\theta_2 = \cos\theta_1 - q/k_1 = \cos\theta_1 \mp \lambda_1/d, \tag{9}$$

where λ_1 is the incident radiation wavelength. If $q > 0$, expression (9) yields the condition $d \geqslant \lambda_1/2$, which limits the grating period from below. The situation with $q < 0$ may occur only at $d \geqslant \lambda_1$.

Now, rewriting (7) in the approximation $\Omega \ll \omega_1$ as

$$\sin\theta_2 = \sin\theta_1 - \beta(\Omega)/k_1 \tag{10}$$

and taking into account (9), we can find the SPP wave vector β:

$$\beta/k_1 = \sin\theta_1 \pm \sqrt{1 - (\cos\theta_1 \mp \lambda_1/d)^2}\,. \tag{11}$$

The wave number β (as well as q) may have two signs; i.e., SPPs may propagate along nanotubes in both positive and negative directions of the z axis. Note that, according to dispersion relations (2), two different SPP propagation directions correspond to different frequencies Ω.

An analysis of all possible combinations of signs for q and β leads to the following results (two cases will be considered).

1. Grating period $d \geqslant \lambda_1$. Figure 3 shows the results of numerical solution of system (2) at d = 2 μm and SWCNT radius a = 1 nm. At $q > 0$, system (2) allows for two solutions. One of them [curve (*1*)] always yields $\beta > 0$, whereas for the other solution [curve (*1′*)], the sign of β changes at the critical value of the angle of incidence (θ_1^{cr}), which gives zero values of β and Ω. Provided that $\Omega \ll \omega_1$, the critical angle is given by the formula

$$\theta_1^{cr} = \arccos(\lambda_1/2d). \tag{12}$$

The values of θ_1^{cr} in formula (12) lie in the range of 60° – 90°. The values of β, corresponding to two solutions, have different signs in the range of $0 \leqslant \theta_1 < \theta_1^{cr}$ and the same (positive) sign at the angle of incidences from the range $\theta_1^{cr} < \theta_1 \leqslant 90°$.

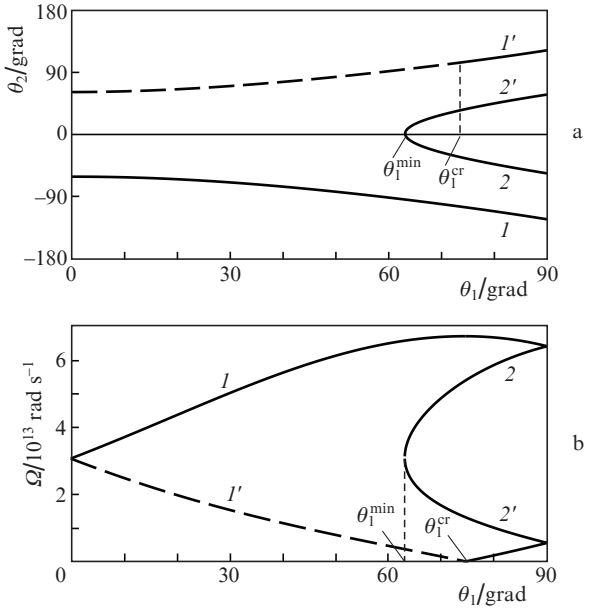

Figure 3. Dependences of (a) the angle θ_2 and (b) frequency Ω on the angle of incidence θ_1 at (*1*, *1′*) $q > 0$ and (*2*, *2′*) $q < 0$; d = 2.0 μm. The solid and dashed lines are the solutions corresponding to $\beta > 0$ and $\beta < 0$, respectively.

The values of the angles θ_2 corresponding to these two solutions differ only in sign: the directions of two diffracted beams are symmetric relative to the x axis. The minimum value of the diffraction angle modulus $\theta_2^{min} = \arccos(1 - \lambda_1/d)$ corresponds to $\theta_1 = 0$, and the maximum value $\theta_2^{max} = \arccos(-\lambda_1/d)$ is implemented at $\theta_1 \to 90°$. Thus, the angles θ_2 may be either acute or obtuse; i.e., the radiation either passes through the structure or reflects from it.

If the angle of incidence θ_1 exceeds the value

$$\theta_1^{min} = \arccos(1 - \lambda_1/d), \tag{13}$$

there may be two more solutions, satisfying the condition $q < 0$ [curves (*2*) and (*2′*) in Fig. 3]. Both solutions give $\beta > 0$, and the two additional diffracted beams are also symmetric relative to the x axis. However, the angle θ_2 for these

beams may be only acute, with a modulus not larger than $\arccos(\lambda_1/d)$. At $\theta_1 = \theta_1^{\min}$, there is only one additional diffracted beam, directed along the x axis.

2. Grating period $\lambda_1/2 < d < \lambda_1$. The results of numerical solution of system (2) are presented in Fig. 4 (the calculations were performed on the assumption that $d = 0.8$ μm and $a = 1$ nm). In this case, there are no solutions with $q < 0$. At $q > 0$, here, as in case 1, we have two solutions and a critical angle, which is determined by the same formula (12) and has the same meaning (its values fall in the range of 0–60°). However, there is also a significant difference: the solutions disappear if the angle of incidence exceeds the maximum allowable value:

$$\theta_1^{\max} = \arccos(\lambda_1/d - 1). \qquad (14)$$

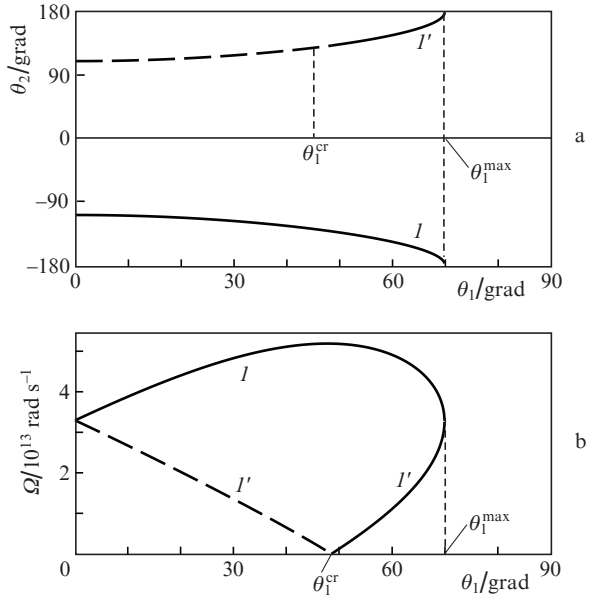

Figure 4. Dependences of (a) the angle θ_2 and (b) frequency Ω on the angle of incidence θ_1 at $d = 0.8$ μm. The solid and dashed lines are the solutions corresponding to $\beta > 0$ and $\beta < 0$, respectively.

At $\theta_1 = \theta_1^{\max}$, two roots merge into one ($\theta_2 = 180°$); i.e., there is one diffracted (reflected) beam, and only one plasmon polariton is excited in each nanotube. This circumstance may help to improve the efficiency of this structure when using it as a THz antenna.

It is fairly difficult to provide a strict periodicity of irradiated structure in the case of a real CNT array. Phase-matching condition (2) can also be satisfied in another situation, where the target is a fairly dense quasi-periodic CNT array, with a distance between nanotubes much smaller than that specified by formula (2). In this case, the phase-matching condition is valid for only those CNTs whose arrangement satisfies (2). Since the emitters satisfying condition (2) are mutually coherent, the intensity of their emission greatly exceeds that of the scattering from other nanotubes. The use of a dense nanotube array makes the requirements to the degree of their order in targets much less stringent.

The conversion efficiency of cw laser radiation into THz radiation (η) for a dense CNT array can be estimated as $\eta = \eta_{\rm pl}\eta_{\rm ant}$, where $\eta_{\rm pl}$ is the laser conversion efficiency into SPPs and $\eta_{\rm ant}$ is the antenna efficiency. Let us assume that the CNT array period on the substrate is d_1 and the period of the nanotubes for which condition (2) is satisfied is d_2 ($d_1 < d_2$). Then, if the incident radiation is entirely absorbed by nanotubes, the order of magnitude of the efficiency $\eta_{\rm pl}$ can be estimated as $(d_1/d_2)^2$; this estimation yields (for typical conditions of the problem) $\eta_{\rm pl} \approx 0.01$.

According to the model of CNT-based dipole antenna, the efficiency of a single antenna $\eta_{\rm ant}$ is 10^{-4}–10^{-6} [17–19, 21]. However, in the case of a CNT array, where many in-phase dipole antennas are excited (the in-phase condition is provided by the laser beam coherence, the efficiency may be much higher and even reach 0.1 [19]. Thus, on the assumption that the electromagnetic wave energy incident on a CNT array is entirely absorbed by SPPs in these nanotubes, the conversion efficiency η may be on the order of $\sim 10^{-3}$; this value corresponds to the limiting theoretical efficiency of the schemes based on the rectification effect [10–13].

A more efficient (although more technically complicated) scheme can be implemented under two-beam-excitation conditions, when two counterpropagating laser beams with slightly different frequencies θ_1 and θ_2 are incident on an SWCNT array at angles ω_1 and ω_2 (Fig. 1b). In this case, the phase-matching condition can be written as

$$k_1 \sin\theta_1 - k_2 \sin\theta_2 = \beta(\Omega). \qquad (15)$$

Here, the SPP generation in a nanotube occurs at the difference frequency $\Omega = \omega_1 - \omega_2$. Condition (15) can be satisfied, for example, by choosing the necessary value of angle θ_2 at a fixed angle of incidence θ_1 of the reference beam. In this case, in contrast to the single-beam excitation, the CNT array periodicity is of no importance, due to which dense CNT arrays can efficiently be used.

5. Conclusions

It was shown that near-IR laser radiation can be used for SPP generation in a periodic CNT array under conditions of single-beam irradiation and for an arbitrarily arranged (aperiodic) array under two-beam-irradiation conditions. Current and voltage standing waves are generated as a result of successive rereflections of the travelling surface wave from the end faces of the plasmonic waveguide formed by the corresponding nanotube. At a specified length L of the plasmonic waveguide, there is a discrete set of frequencies for which the standing-wave formation condition is satisfied: $\beta(\Omega)L = m\pi$, where m is an integer. Thus, due to the implemented geometric resonances, the plasmonic waveguide considered here can be used as an antenna emitting in the THz and far-IR ranges.

We should emphasise that in the case under consideration resonances should be observed for wavelengths that may significantly exceed (by several orders of magnitude) the sizes of the corresponding antenna in a free space, which is explained by the strong delay of THz and far-IR SPPs. Note also that the SPP frequency in this scheme can easily be tuned by varying the laser beam angle of incidence. This tuning must be performed to satisfy the geometric resonance condition, which provides a sharp increase in the antenna efficiency.

Acknowledgements. This study was supported by the Ministry of Education and Science of the Russian Federation (Project Nos 14.Z50.31.0015, 16.2773.2017/4.6, 3.5698.2017/9.10, and 3.3889.2017/4.6), the Russian Foundation for Basic Research

(Project No. 17-0201382), and the Russian Science Foundation (Project No. 18-12-00457).

References

1. Lee Y.S. *Principles of Terahertz Science and Technology* (New York: Springer, 2009).
2. Bratman V.L., Litvak A.G., Suvorov E.V. *Phys. Usp.*, **54**, 837 (2011) [*Usp. Fiz. Nauk*, **181**, 867 (2011)].
3. Zhang X.-C., Xu J. *Introduction to THz Wave Photonics* (New York: Springer, 2010).
4. Tonouchi M. *Nat. Photonics*, **1**, 97 (2007).
5. Weide D. *Opt. Photon. News*, **14**, 49 (2003).
6. Aleshkin V.Ya., Antonov A.A., Gaponov S.V., Dubinov A.A., Krasil'nik Z.F., Kudryavtsev K.E., Spivakov A.G., Yablonskii A.N. *JETP Lett*., **88**, 787 (2009) [*Pis'ma Zh. Eksp. Teor. Fiz*., **88**, 905 (2008)].
7. Faist J., Capasso F., Sivco D., Sirtori C., Hutchinson A.L., Cho A.Y. *Science*, **264**, 553 (1994).
8. Lewis R.A. *J. Phys. D*, **47**, 374001 (2014).
9. Leyman R.R., Gorodetsky A., Bazieva N., Molis G., Krotkus A., Clarke E., Rafailov E.U. *Laser Photon. Rev*., **10**, 772 (2016).
10. Sazonov C.V. *Izv. Akad. Nauk SSSR, Ser. Fiz*., **78**, 296 (2014).
11. Bugay A.N., Sazonov S.V. *Phys. Lett. A*, **374**, 1093 (2010).
12. Fülöp J.A., Pálfalvi L., Klingebiel S., Almási G., Krausz F., Karsch S., Hebling J. *Opt. Lett*., **37**, 557 (2012).
13. Nagai M., Matsubara E., Ashida M. *Opt. Express*, **20**, 6509 (2012).
14. Sharma S., Vijay A. *Phys. Plasmas*, **25**, 023114 (2018).
15. Slepyan G.Ya., Maksimenko S.A., Lakhtakia A., Yevtushenko O.M., Gusakov A.V. *Phys. Rev. B*, **60**, 17136 (1999).
16. Kibis O.V., Parfitt D.G.W., Portnoi M.E. *Phys. Rev. B*, **71**, 035411 (2005).
17. Hanson G.W. *IEEE Trans. Ant. Prop*., **53**, 3426 (2005).
18. Hao J., Hanson G.W. *Phys. Rev. B*, **74**, 035119 (2006).
19. Shuba M.V., Slepyan G.Ya., Maksimenko S.A., Thomsen C., Lakhtakia A. *Phys. Rev. B*, **79**, 155403 (2009).
20. Batrakov K.G., Maksimenko S.A., Kuzhir P.P., Thomsen C. *Phys. Rev. B*, **79**, 125408 (2009).
21. D'yachkov P.N., Bochkov I.A. *Nauch. Tekh. Vedomosti SPbPU, Estestv. Inzh. Nauki*, **146**, 85 (2012).
22. Sadykov N.R., Skorkin N.A. *Zh. Tekh. Fiz*., **83**, 1 (2013).
23. Bulyarskii S.V., Dudin A.A., Orlov A.P., Pavlov A.A., Leont'ev V.L. *Zh. Tekh. Fiz*., **87**, 1624 (2017).
24. Chepurnov A.S., Ionidi V.Y., Kirsanov M.A., Kitsyuk E.P., Klenin A.A., Kubankin A.S., Oleinik A.N., Pavlov A.A., Shchagin A.V. *J. Phys.: Conf. Ser*., **934**, 012013 (2017).
25. Atdaev A., Danilyuk A.L., Labunov V.A., Prishchepa S.L., Pavlov A.A., Basaev A.S., Shaman Yu.P. *Izv. Vyssh. Uchebn. Zaved., Ser. Electron*., **20**, 357 (2015).
26. Polokhin A.A., Gerasimenko A.Yu., Dudin A.A., Ichkitidze L.P., Kitsyuk E.P., Orlov A.P., Pavlov A.A., Shaman Yu.P. *Kratk. Soobshch. Fiz. FIAN*, (44), 42 (2017).
27. Kadochkin A.S., Moiseev S.G., Dadoenkova Y.S., Svetukhin V.V., Zolotovskii I.O. *Opt. Express*, **25**, 27165 (2017).
28. Moradi A. *Photonics and Nanostructures*, **11**, 85 (2013).
29. Moradi A. *J. Electromagnetic Analysis & Applications*, **2**, 672 (2010).
30. Martin-Moreno L., Garcia de Abajo F.J., Garcia-Vidal F.J. *Phys. Rev. Lett*., **115**, 173601 (2015).
31. Attiya A.M. *Prog. Electromagn. Res*., **94**, 419 (2009).
32. Nakanishi T., Ando T. *J. Phys. Soc. Jap*., **78**, 114708 (2009).
33. Sasaki K., Murakami Sh., Yamamoto H. *Appl. Phys. Lett*., **108**, 163109 (2016).
34. Miano G., Villone F. *IEEE Trans. Ant. Prop*., **54**, 2713 (2006).